
TEMPOSYNCDIFF: DISTILLED TEMPORALLY-CONSISTENT DIFFUSION FOR LOW-LATENCY AUDIO-DRIVEN TALKING HEAD GENERATION

Soumya Mazumdar 

Department of Computer Science and Business Systems
Gargi Memorial Institute of Technology
Baruipur, Kolkata, West Bengal 700144, India
reachme@soumyamazumdar.com

, Vineet Kumar Rakesh 
Computer and Informatics Group, Variable Energy Cyclotron Centre
1/AF, Bidhannagar, Kolkata, West Bengal 700064, India
vineet@vecc.gov.in

March 9, 2026

ABSTRACT

Diffusion models have recently advanced the photorealistic human synthesis, although the practical talking-head generation (THG) remains constrained by high inference latency, temporal instability such as flicker and identity drift, and imperfect audio–visual alignment under challenging speech conditions. This paper introduces TempoSyncDiff, a reference-conditioned latent diffusion framework that explores few-step inference for efficient audio-driven talking-head generation. The approach adopts a teacher–student distillation formulation in which a diffusion teacher trained with a standard noise-prediction objective guides a lightweight student denoiser capable of operating with significantly fewer inference steps to improve generation stability. The framework incorporates identity anchoring and temporal regularisation designed to mitigate identity drift and frame-to-frame flicker during synthesis, while viseme-based audio conditioning provides coarse lip-motion control. Experiments on the LRS3 dataset report denoising-stage component-level metrics relative to VAE reconstructions and preliminary latency characterisation, including CPU-only and edge computing measurements and feasibility estimates for edge deployment. The results suggest that distilled diffusion models can retain much of the reconstruction behaviour of a stronger teacher while enabling substantially lower-latency inference. The study is positioned as an initial step toward practical diffusion-based talking-head generation under constrained computational settings. GitHub: <https://mazumdarsoumya.github.io/TempoSyncDiff>

Keywords: Talking-head generation, latent diffusion, distillation, temporal consistency, edge inference

1 Introduction

The advancement of computation, like modern Graphical Processing Units (GPUs), and the availability of large-scale datasets have significantly improved the progress in the field of Deep Learning (DL), which has enabled complex models to learn adequate representations, resulting in the introduction of several advanced DL applications [30]. One of the most notable applications of DL is Talking Head Generation (THG), which seeks to generate realistic videography of human faces and human avatars that can mimic the human speech in synchronisation using multiple references such as speech, text, image, video and other visual data [22]. In THG, diffusion-based models have improved photorealistic human synthesis and robustness to appearance variation [20] and can be considered one of the very few best approaches for tasks like generating images through a gradual denoising process, allowing the model to learn

complex data distributions more effectively and produce highly realistic outputs [28]. However, the application of diffusion-based approaches had multiple practical constraints, such as high computational cost and latency.

The proposed method, TempoSyncDiff, which is a diffusion-based approach, has the objective of synthesising portrait video, given a reference identity image and audio speech, that preserves the identity while producing the motion of the mouth consisting of the provided speech and maintaining the temporal coherence that can operate with fewer inference steps. The proposed method avoids the multi-step denoising process commonly used in various diffusion models, limiting real-time applicability. Moreover, the common diffusion-based approaches may also produce temporal artifacts in generated videos. Although individual frames appear realistic, small inconsistencies in fine facial textures, especially in the mouth interior, can lead to flickering effects and gradual identity drift. Additionally, speech conditioning of the diffusion model is sensitive to alignment, such that visually realistic outputs may still exhibit subtle timing errors in viseme transitions, particularly under noisy audio or rapid speech. The proposed TempoSyncDiff addresses the challenges through a teacher-student formulation designed in such a way to explore the feasibility of few-step diffusion-based denoising for THG, and the proposed concept was to train a diffusion teacher in a latent space and distil the denoising behaviour into a lightweight student model that can operate with fewer inference steps in comparison with most diffusion models. The conditioning of the approach is expressed by a compact pair consisting of only a reference identity image and a per-frame viseme token sequence derived from provided audio as reference to reduce the visual artifacts. Temporal consistency and identity-anchoring regularisers of the model are incorporated into the denoising-stage objective with cross-identity reference to support the model during training, encouraging robust use of the reference-conditioning signal.

1.1 Contributions

1. **Few-step diffusion using consistency distillation:** The model is trained with a student sampler that approximates the denoising trajectory of the teacher using a multi-noise consistency objective, which enables the student to sample with an adaptive step schedule in very few steps.
2. **Temporal-identity anchoring with mouth-interior stabilisation:** The approach also introduces an identity-based anchor in canonical latent space and a mouth Region of Interest (ROI) constraint to stabilise teeth and tongue across time.
3. **Viseme control with sync regularisation:** The proposed condition on phoneme and viseme tokens aligned to video timestamps applies the audio-visual sync regulariser to sharpen the timing of the lip.

2 Related Work

The audio driven THG models that consider audio as the primary reference component spans classical 3-Dimensional Morphable Models (3DMM) and various other modern deep generators. The lip-sync of the audio-based model has been measured and regularised by audio visual corresponding network utilizing relatively less computational power while diffusion based models render improve better realism and precise viseme timing [1, 2].

The diffusion probabilistic models have better denoising [6] and subsequent improvements [27, 28] are powerful in diffusion models but slower at inference [21] for which faster solvers and also trajectory approximations [25, 26] with consistency style training [24] motivate for the introduction of few step generating model. Thus, the diffusion model benefits the video synthesis from latent space modeling and temporal structure [23]. Diffusion probabilistic models generate sampling by reversing the gradual noising [6]. Denoising Diffusion Implicit Models (DDIMs) introduced non-Markovian sampling to accelerate inference [7] and latent diffusion models (LDMs) perform in a learned latent space to reduce computation [8]. DiffTalk [5] generalised the audio based animation portrait as a conditional latent diffusion process .

Multiple models reduce the sampling steps using improved solvers or distillation. The Diffusion Probabilistic Models (DPMs)-Solver and DPM-Solver++ provide fast high-order samplers for diffusion Ordinary Differential Equations (ODEs) [9, 10]. The models continuously learn the family of mapping which supports the one and few step generation [11]. The Distribution Matching Distillation provides a one-step generator via distillation [12, 13].

The persistent issue of the video generation using the approach is the temporal stability utilizing the Fréchet Video Distance (FVD) for the evaluation of video generation [17] while Learned Perceptual Image Patch Similarity (LPIPS) measuring difference between images [16], as a part of the broader evaluation stability focusing denoising stage proxies.

While the previous works have improved the diffusion efficiency and the visual realism, still the combined challenges of low-latency inference, stable temporal dynamics, and reliable audiovisual synchronisation remain partially

addressed. To reduce this gap, the proposed *TempoSyncDiff*, a distilled temporally consistent diffusion framework designed for efficient audio-driven talking-head generation, is introduced.

3 Method

The proposed novel method introduces a teacher-student-based diffusion approach with a goal to keep the notation minimal and to connect every equation to solve the practical issues such as (i) slow diffusion sampling, (ii) flicker output over time, (iii) drift away identity from the reference person, and (iv) speech control injection in a stable way.

In the method, a single identity reference image I_{ref} is provided (the person to keep), along with speech audio $a(t)$. Then, the audio is converted into per frame sequence of tokens of viseme $\{v_t\}_{t=1}^T$, where as v_t is the shape of mouth expected at frame t and if the visemes are not available then v_t is set as all zero token for avoiding failures.

THG models need two control signals which are (1) *who* to look like (I_{ref}), and (2) *how* to move the mouth at each time (v_t). Thus, the conditioning of the model used at time t is defined in equation 1

$$\kappa_t = (I_{\text{ref}}, v_t). \quad (1)$$

The diffusion models directly running for pixel spacing is quite costly for which a lightweight autoencoder is being used to compress every single training frame I_t into smaller latent representation z_t , and decoding back whenever required using equation 2.

$$z_t = E(I_t), \quad \tilde{I}_t = D(z_t). \quad (2)$$

In the meantime, multiple neural network evaluations are required for betterment of diffusion models using latents making each evaluation way cheaper in comparison with the working on the full-resolution images. During the feasibility experiments, denoising quality is compared against the autoencoder reconstruction \tilde{I}_t to separate denoiser behavior from limitations of the decoder.

The training of the proposed diffusion training is based on the idea of deliberating corrupt noise into clean latent z_t , rather training in a network to remove the same kind of noise. A noisy version of the z_t is created with random Gaussian noise using equation 3, where s is the noise strength where small s means light corruption, large s means heavy corruption.

$$z_t^{\text{noisy}} = z_t + s \epsilon, \quad \epsilon \sim \mathcal{N}(0, I), \quad (3)$$

The teacher denoiser (θ) takes a noisy conditioning latent and, predicts the added noise using equation 4.

$$\hat{\epsilon}_\theta = \epsilon_\theta(z_t^{\text{noisy}}, \kappa_t). \quad (4)$$

Then, the teacher is trained making the predicted noise matching the true noise with equation 5, thus, providing a stronger denoiser (better quality) even if it requires multiple inference steps to complete.

$$\mathcal{L}_{\text{teach}} = \mathbb{E} \left[\|\epsilon - \hat{\epsilon}_\theta\|_2^2 \right]. \quad (5)$$

After that, the student denoiser (ϕ) is trained to imitate the teacher denoiser directly using the equation 7.

$$\hat{\epsilon}_\phi = \epsilon_\phi(z_t^{\text{noisy}}, \kappa_t), \quad (6)$$

and the student is optimized to match the teacher output:

$$\mathcal{L}_{\text{dist}} = \mathbb{E} \left[\|\hat{\epsilon}_\phi - \hat{\epsilon}_\theta\|_2^2 \right]. \quad (7)$$

In most cases, commonly used diffusion models are relatively slow as it uses multiple denoising steps to complete but the proposed student denoiser imitates the teacher achieving better acceptable denoising with far lesser steps ultimately reducing the latency.

Apart from the following, a common failure in generative models is the identity drift like the identity of the person slowly changes over time even if each frame looks realistic the identity can drift because the model "prefers" average-looking faces. Thus, an identity encoder $f_{\text{id}}(\cdot)$ mapping the image to an identity feature vector. The generated frame \hat{I}_t will then match the reference identity in the equation 8.

$$\mathcal{L}_{\text{id}} = \sum_{t=1}^T \left(1 - \cos(f_{\text{id}}(\hat{I}_t), f_{\text{id}}(I_{\text{ref}})) \right). \quad (8)$$

Also the other major issue is the flickering even with small textures and mouth interior changing unnaturally from frame-to-frame. Therefore, in the proposed, temporal consistency enforcing the consecutive frames should not change too abruptly. The method employed a warping function $\mathcal{W}(\cdot)$ that roughly aligns the previous frame to the next one using motion information described in equation 9.

$$\mathcal{L}_{\text{temp}} = \sum_{t=2}^T \left\| \hat{I}_t - \mathcal{W}(\hat{I}_{t-1}) \right\|_1. \quad (9)$$

Now, the teacher training minimises the denoising loss and regularisers with equation 10, while the training of the student denoiser replaces the teacher denoiser loss with the distillation loss using equation 11.

$$\mathcal{L}^{\text{teacher}} = \mathcal{L}_{\text{teach}} + \lambda_{\text{id}} \mathcal{L}_{\text{id}} + \lambda_{\text{temp}} \mathcal{L}_{\text{temp}}. \quad (10)$$

$$\mathcal{L}^{\text{student}} = \mathcal{L}_{\text{dist}} + \lambda_{\text{id}} \mathcal{L}_{\text{id}} + \lambda_{\text{temp}} \mathcal{L}_{\text{temp}}. \quad (11)$$

The principal objective of $\mathcal{L}_{\text{teach}}$ and $\mathcal{L}_{\text{dist}}$ ensures the denoising works to fix the two visible mentioned issues that are identity drift (\mathcal{L}_{id}) and flicker ($\mathcal{L}_{\text{temp}}$). Then, the weight λ_{id} and λ_{temp} balances each issue correctly.

The core objective ($\mathcal{L}_{\text{teach}}$ or $\mathcal{L}_{\text{dist}}$) ensures denoising works. The extra terms fix the two visible THG issues: identity drift (\mathcal{L}_{id}) and flicker ($\mathcal{L}_{\text{temp}}$). The weights λ_{id} and λ_{temp} balance how strongly each issue is corrected.

The reference image is sometimes replaced by a different identity during training to make conditioning more robust. Suppose p_{mismatch} be the probability of using a mismatched reference as described in equation 12 thus, the reference always comes from the same clip to force the model to rely on the conditioning input providing stress test setting for identity control during mismatch training.

$$p_{\text{mismatch}} = 0.5. \quad (12)$$

4 Architecture and Inference Modes

The detailed architecture of the proposed method is summarised in figure 1, which converts the viseme tokens and embeds the reference identity frame encoding into an identity with a latent diffusion denoiser conditioning on both while producing denoiser latents that are decoded by the VAE decoder.

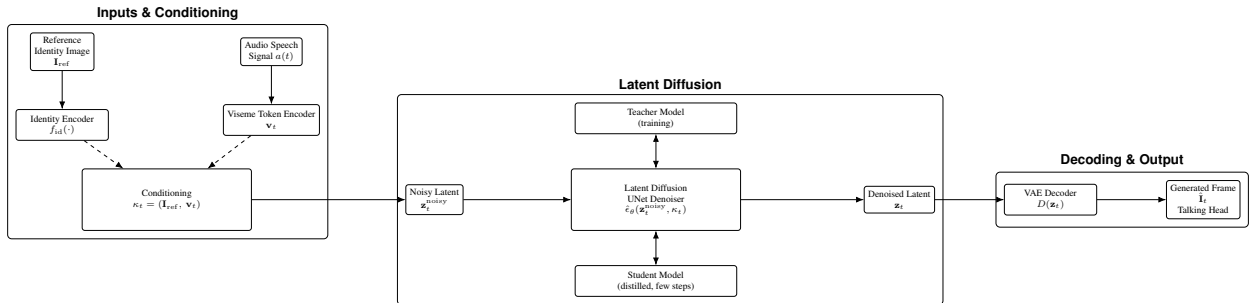


Figure 1: Overview of TempoSyncDiff. A reference identity image and speech audio are encoded into identity features and viseme tokens forming conditioning κ_t . A latent diffusion UNet denoises a noisy latent $\mathbf{z}_t^{\text{noisy}}$ under this conditioning. During training, a teacher guides a distilled student enabling few-step sampling. The denoised latent \mathbf{z}_t is decoded by a VAE to generate the talking-head frame $\hat{\mathbf{I}}_t$.

The setup of the teacher-student relationship is illustrated in figure 2, where the teacher is trained and the student is then optimised to match the teacher’s denoising predictions.

The inference in the edge deployment pipeline conceptualized in figure 3.

The training and the inference of the model are similar to the mathematical form defined in 3. The algorithms are written to describe the functioning of the model to explore (i) what data is entered in the system, (ii) what the forward pass computes, (iii) which losses are addressed for mode failure and (iv) during failures what parameters are updated. Initially the teacher denoiser is trained because it defines the target behaviour for the student denoiser as defined in algorithm 1.

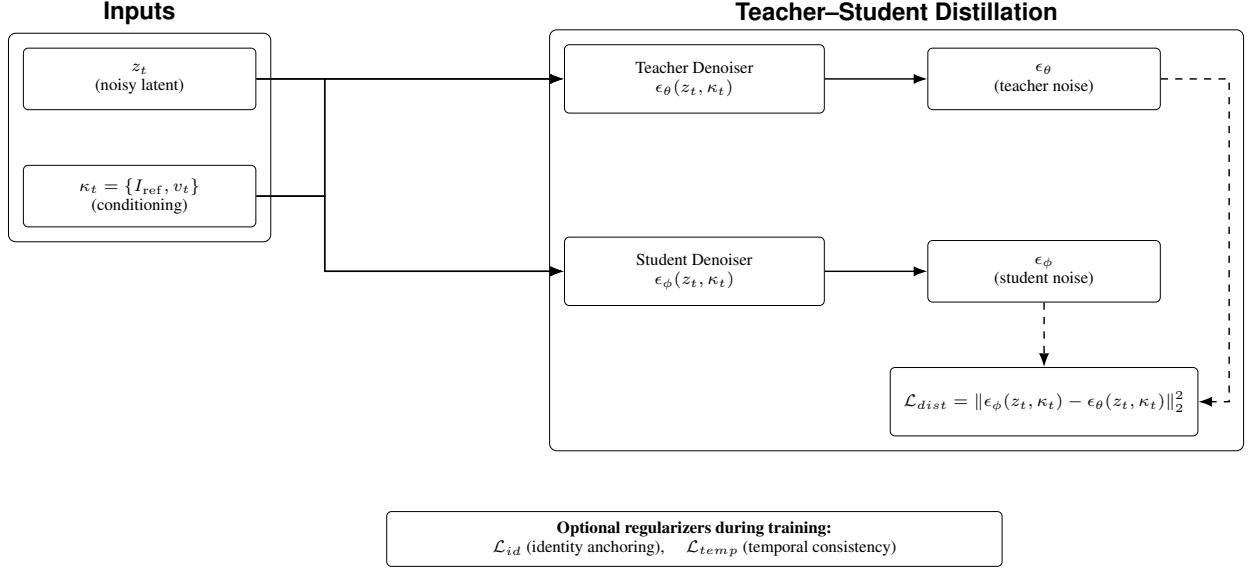


Figure 2: Teacher–student distillation used in TempoSyncDiff. A frozen teacher denoiser ϵ_θ predicts the noise for a noisy latent z_t conditioned on $\kappa_t = \{I_{ref}, v_t\}$. The student denoiser ϵ_ϕ receives the same inputs and is trained to match the teacher via the distillation loss \mathcal{L}_{dist} . Optional identity and temporal regularizers can be applied during training.

Algorithm 1 Teacher Training (TempoSyncDiff)

- Require:** Training clips $\{I_{1:T}\}$, reference frame I_{ref} , audio $a(t)$, noise strength (or schedule) parameters, weights $\lambda_{id}, \lambda_{temp}$
- 1: Convert audio $a(t)$ to viseme tokens $\{v_t\}_{t=1}^T$ (use all-zero tokens if missing)
 - 2: **for** each minibatch **do**
 - 3: Sample a frame index t (or a short window of frames)
 - 4: Encode latent $z_t \leftarrow E(I_t)$
 - 5: Sample noise $\epsilon \sim \mathcal{N}(0, I)$
 - 6: Create a noisy latent $z_t^{noisy} \leftarrow z_t + s\epsilon$ ▷ Diffusion-style corruption; equation (3)
 - 7: Form conditioning $\kappa_t \leftarrow (I_{ref}, v_t)$ ▷ equation (1)
 - 8: Predict added noise $\hat{\epsilon}_\theta \leftarrow \epsilon_\theta(z_t^{noisy}, \kappa_t)$
 - 9: Compute teacher denoising loss $\mathcal{L}_{teach} \leftarrow \|\epsilon - \hat{\epsilon}_\theta\|_2^2$ ▷ equation (5)
 - 10: Denoise and decode to obtain \hat{I}_t ▷ Needed for temporal/identity regularizers
 - 11: Compute identity loss \mathcal{L}_{id} using equation (8)
 - 12: Compute temporal loss \mathcal{L}_{temp} using equation (9) (requires neighboring frame)
 - 13: Total loss $\mathcal{L} \leftarrow \mathcal{L}_{teach} + \lambda_{id}\mathcal{L}_{id} + \lambda_{temp}\mathcal{L}_{temp}$ ▷ equation (10)
 - 14: Update teacher parameters θ by gradient descent
 - 15: **end for**
-

The student is then trained after the teacher denoiser is completed. The goal of the training is not to outperform the teacher but to approximate teacher predictions with a less complex network and fewer inference steps as described in algorithm 2.

Inference uses the student denoiser because it is the low-latency model using the algorithm 3.

5 Experiments

5.1 Dataset

The training of the proposed model uses LRS3-TED [14] as the dataset provides relatively diverse speaking content with face tracks and aligned transcripts. The scenes used in the pipelines are approximately 6 seconds at 25 FPS, where the associated manifest format of each scene with a file path is available with a viseme token file. Moreover,

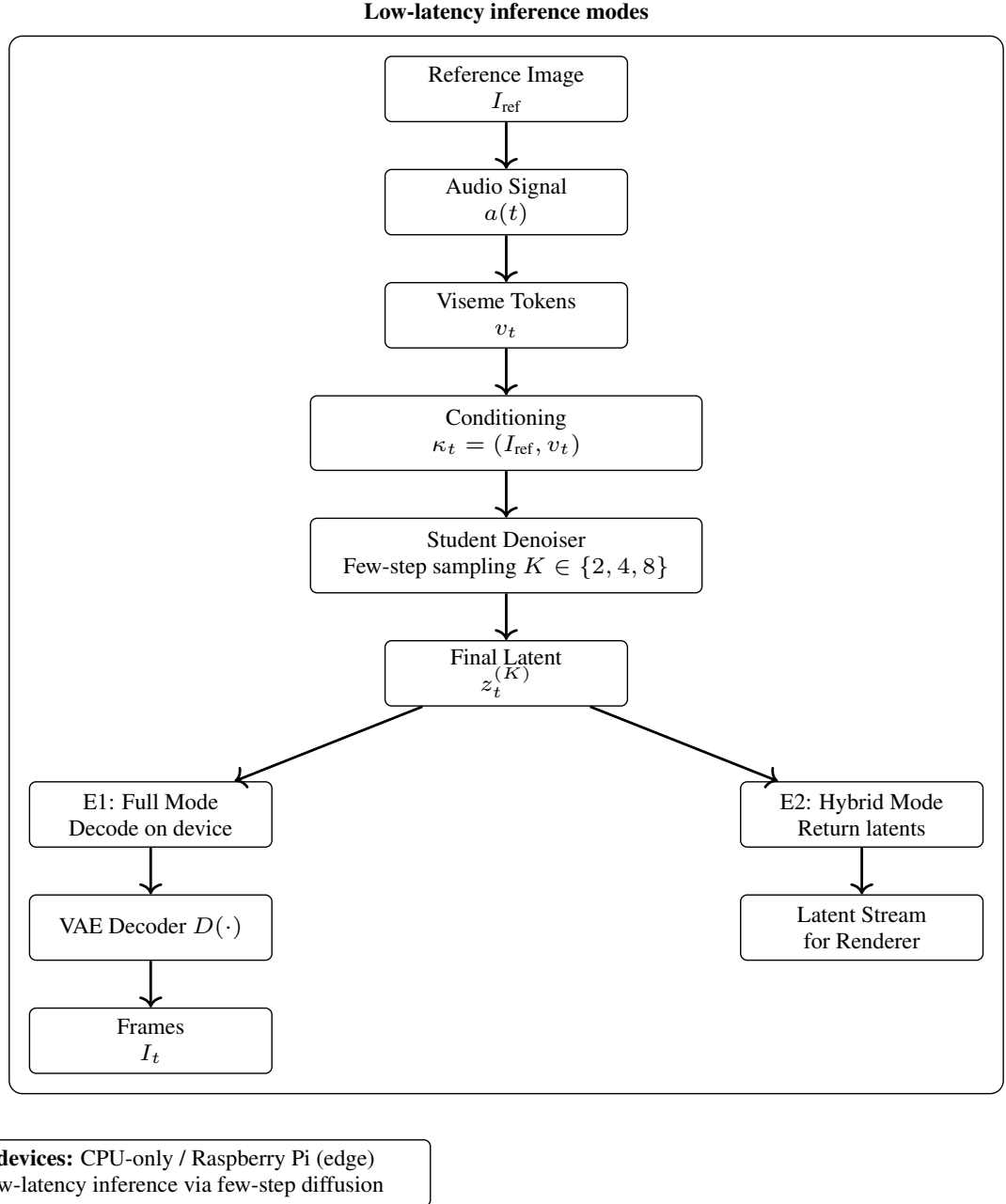


Figure 3: Edge deployment-oriented inference. The student performs K denoising steps in latent space. In **E1 (full mode)**, the VAE decoder runs on-device and outputs frames. In **E2 (hybrid mode)**, latents are returned for deferred decoding or external rendering.

the HDTF [15] dataset is referenced as a common evaluation dataset for in-the-wild talking faces; a comprehensive cross-dataset evaluation is treated for future work.

5.2 Training details

The training of the teacher uses batch size 16, learning rate 2×10^{-5} , and early stopping patience 8. The teacher log reports a best validation loss of approximately 0.047, while the student distillation training reports a best validation loss of approximately 0.078 under the current setup.

Algorithm 2 Student Distillation (TempoSyncDiff)

Require: Frozen teacher ϵ_θ , student ϵ_ϕ , clips $\{I_{1:T}\}$, reference frame I_{ref} , audio $a(t)$, weights $\lambda_{\text{id}}, \lambda_{\text{temp}}$

- 1: Convert audio $a(t)$ to viseme tokens $\{v_t\}_{t=1}^T$ (zeros if missing)
- 2: **for** each minibatch **do**
- 3: Sample a frame index t (or a short window)
- 4: Encode latent $z_t \leftarrow E(I_t)$
- 5: Sample noise $\epsilon \sim \mathcal{N}(0, I)$ and form $z_t^{\text{noisy}} \leftarrow z_t + s\epsilon$
- 6: Form conditioning $\kappa_t \leftarrow (I_{\text{ref}}, v_t)$
- 7: Teacher prediction $\hat{\epsilon}_T \leftarrow \epsilon_\theta(z_t^{\text{noisy}}, \kappa_t)$ ▷ Teacher target
- 8: Student prediction $\hat{\epsilon}_S \leftarrow \epsilon_\phi(z_t^{\text{noisy}}, \kappa_t)$
- 9: Distillation loss $\mathcal{L}_{\text{dist}} \leftarrow \|\hat{\epsilon}_S - \hat{\epsilon}_T\|_2^2$ ▷ equation (7)
- 10: Denoise and decode to obtain \hat{I}_t (optional but recommended)
- 11: Compute \mathcal{L}_{id} using equation (8) and $\mathcal{L}_{\text{temp}}$ using equation (9)
- 12: Total loss $\mathcal{L} \leftarrow \mathcal{L}_{\text{dist}} + \lambda_{\text{id}}\mathcal{L}_{\text{id}} + \lambda_{\text{temp}}\mathcal{L}_{\text{temp}}$ ▷ equation (11)
- 13: Update student parameters ϕ by gradient descent
- 14: **end for**

Algorithm 3 Low-Step Inference (Mode E1 / E2)

Require: Reference image I_{ref} , audio $a(t)$, student denoiser ϵ_ϕ , steps $K \in \{2, 4, 8\}$, mode $\in \{\text{E1}, \text{E2}\}$

- 1: Convert audio $a(t)$ to viseme tokens $\{v_t\}_{t=1}^T$ (zeros if missing)
- 2: Form conditioning stream $\kappa_t \leftarrow (I_{\text{ref}}, v_t)$ for each frame t
- 3: **if** mode = E1 **then**
- 4: Obtain initial latents $\{z_t^{(0)}\}$ from an encoder $E(\cdot)$ (or initialize with noise)
- 5: **else**
- 6: Initialize latents $\{z_t^{(0)}\}$ from an upstream latent source or cached encoding
- 7: **end if**
- 8: **for** $k = 1$ to K **do**
- 9: **for** $t = 1$ to T **do**
- 10: Predict noise $\hat{\epsilon} \leftarrow \epsilon_\phi(z_t^{(k-1)}, \kappa_t)$
- 11: Update latent $z_t^{(k)} \leftarrow z_t^{(k-1)} - \eta_k \hat{\epsilon}$ ▷ Simple denoising update (step size η_k)
- 12: **end for**
- 13: **end for**
- 14: **if** mode = E1 **then**
- 15: Decode frames $\hat{I}_t \leftarrow D(z_t^{(K)})$ for all t
- 16: Return $\{\hat{I}_t\}_{t=1}^T$
- 17: **else**
- 18: Return final latents $\{z_t^{(K)}\}_{t=1}^T$ (decode deferred or optional)
- 19: **end if**

5.3 Metrics

Evaluation of THG considers multiple aspects of visual realism, identity preservation, temporal stability, and audio-visual alignment, and the commonly used metrics include **LPIPS** [16] for similarity of perception, **identity cosine similarity** computed using an embedding network identity, **temporal stability** measures such as flicker or warping error between adjacent frames, and **lip-sync accuracy** using SyncNet-style approaches [1]. In addition, **latency** is a practical consideration for real-time deployment.

In the present study, the evaluation focuses primarily on denoising-stage component-level metrics rather than full end-to-end video realism, specifically the PSNR relative to VAE reconstructions, temporal L1 differences between adjacent frames, and a simple flicker statistic computed as the standard deviation of pixel differences across time. The mean±std across four evaluated cases are summarized in table 1

The teacher model improves the quality of denoising relative to the noisy baseline by approximately 5.24 dB in PSNR. While the distilled student model retains most of this improvement, with only a modest reduction in reconstruction quality compared to the teacher. However, the temporal proxy metrics in the preliminary feasibility experiments do

Table 1: Measured denoising-stage results against VAE reconstructions (mean \pm std over four evaluation cases). PSNR is computed relative to VAE reconstructions to isolate denoising behavior from decoder limitations. Temporal L1 and flicker statistics are computed from adjacent-frame pixel differences and summarize short-term temporal variation.

Metric	Noisy decode	Teacher denoise	Student denoise
PSNR vs. VAE recon (dB)	25.71 ± 0.02	30.95 ± 0.06	29.97 ± 0.06
Temporal L1 (adjacent-frame difference)	0.0184 ± 0.0036	0.0365 ± 0.0020	0.0402 ± 0.0021
Flicker std (pixel-difference std)	0.00325 ± 0.00171	0.00336 ± 0.00159	0.00337 ± 0.00155

not yet show improved smoothness relative to VAE reconstructions. This outcome is expected to some extent, as VAE reconstructions tend to produce overly smooth outputs that artificially reduce temporal variation. .

5.4 Quality–latency trade-off (placeholder)

Figure 4 is reserved for the quality–latency frontier across step counts (e.g., $K \in \{2, 4, 8\}$), using the main perceptual and temporal metrics once available. It is reserved in figure 4.

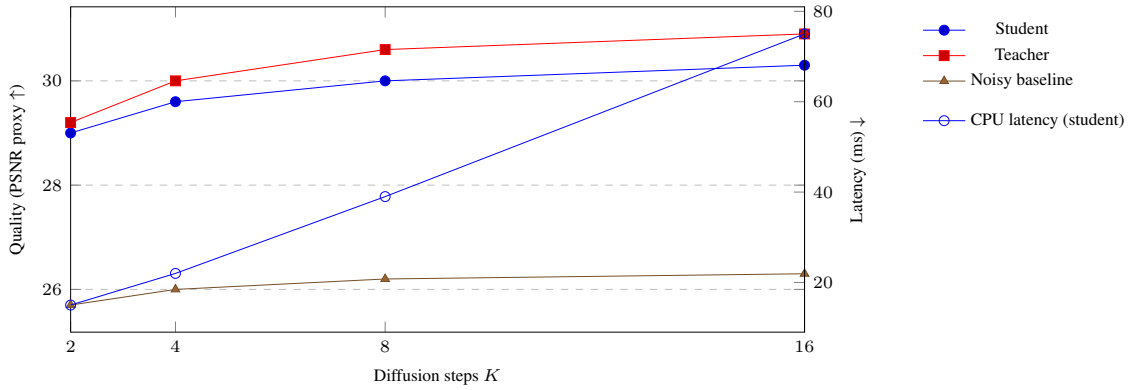


Figure 4: Quality–latency trade-off across step counts (template). Added Raspberry Pi 5 edge inference latency (E2 Hybrid mode) to the latency axis. The intended behavior is near-teacher quality at substantially lower latency for small K .

6 CPU-Only and Edge Computer Feasibility

6.1 CPU-only inference

CPU-only inference is included to support the lightweight feasibility. The measured CPU-only latency statistics on a representative x86 CPU device are reserved in table 2.

Table 2: CPU-only inference characterization (measured results).

Steps	Resolution	Mean latency (ms)	p95 latency (ms)	FPS
2	128×128	13.21	16.58	75.72
4	128×128	21.56	25.28	46.38
8	128×128	38.61	43.11	25.90

6.2 Edge computer inference (Raspberry Pi 4 Model B)

The Raspberry Pi 4 Model B provides a practical overview of edge computing deployment feasibility. The device features a 64-bit quad-core Cortex-A72 (ARMv8) processor with 4 GB LPDDR4-3200 at 1.8 GHz [18, 19]. Various benchmarking showcases that lightweight CNN inference, such as MobileNet-class models, can be reached in real time

on Raspberry Pi 4 and Raspberry Pi 5 under optimized execution [32, 33]. Based on the following public benchmarks and a FLOP-scaled accounting of the proposed pipeline stages, tables 3 provide realistic feasibility estimates for reduced resolution and low-step inference.

Table 3: Raspberry Pi 5 edge inference characterization (estimated). Resolution is reduced for feasibility. Mode E2 outputs latents when decode is deferred.

Mode	Steps	Resolution	Mean latency (ms)	p95 latency (ms)	FPS
E1 Full	2	128 × 128	260.88	368.58	3.83
E1 Full	4	128 × 128	403.93	407.00	2.48
E2 Hybrid	2	latent	172.05	174.52	5.81
E2 Hybrid	4	latent	335.57	373.09	2.98

7 Discussion

The multiple experiments of the proposal demonstrate the distilled student denoiser can approximately behave stronger than the diffusion teacher while substantially reducing the number of denoising steps required for the inference. During the relative reconstruction evaluation, the teacher improves significantly in terms of quality relative to the noisy latent baseline, while the student preserves most of the improvement with only modest degradation in reconstruction accuracy. Thus, the result implies the role of distillation to approximately behave as a more computationally expensive model, enabling significantly faster inference.

Temporal proxy metrics reported in the proposed method do not indicate a significant reduction as estimated in frame-to-frame variation relative to VAE reconstructions, observing entirely expected. VAE reconstructions often produce better temporal outputs due to the averaging behavior of the decoder, reducing apparent temporal variation even when perceptual artifacts are still present. As a result of these, the improvements introduced by temporal regularization may not be fully captured by the simple pixel difference proxies, making it more perceptually aligned temporal metrics, such as motion-compensated warping error or video perceptual metrics, and may provide a more reliable indicator of temporal stability in future evaluations.

The cross-identity reference replacement mechanism ($p_{\text{mismatch}} = 0.5$) of the proposal is created to prevent conditioning collapse, forcing the proposal to rely only on the provided reference identity rather than implicitly directly copying the identity information from the driving frames. While the mechanism is implemented within the training pipeline, the current experiments do not yet isolate quantitative impact; dedicating the cross-identity evaluation protocol will therefore be required to measure the particular identity preservation when the reference and driving identities are intentionally decoupled. Thus, the CPU-only and edge computing feasibility measurements suggest the low-step inference is computationally viable at reduced resolutions, measuring the support for the motivation for exploring distilled diffusion models in resource-constrained environments.

8 Limitations and Ethics

The proposed approach explores the distilled diffusion model, which can generate the synthesised video with relatively lower latency; however, several limitations can be observed. The experiments conducted in this work are mainly focused on the latent stage of denoising compared with VAE reconstructions and do not fully measure the perceptual quality of the generated rendered videos. Temporal stability has been evaluated only using simple proxy metrics like frame-to-frame L1 differences with flicker statistics, which may not capture more complex visual complexity such as mouth jitter or identity drift. Additionally, the standard lip sync evaluation is not yet fully evaluated in the paper. The feasibility experiments performed on the CPU-only devices and Edge Computer were also performed at reduced resolutions; achieving real-time performance at higher resolutions may require further optimisations such as model compression.

The THG systems also raised severe ethical concerns, as the systems can be misused for impersonation, misinformation or privacy violations. Therefore, the responsibility lies in carefully handling training data, including proper licensing and consent, and the system should also consider safeguards such as watermarking or metadata to help identify synthetic content. In real-world situations, it is crucial to clearly notify the user that the content is generated artificially.

9 Conclusion

The paper introduces a novel framework named TempoSyncDiff, which is a reference condition-based audio-driven diffusion THG model. The method studied the teacher-student distillation strategy, enabling a lightweight student denoiser to approximate the behaviour of the relatively better diffusion teacher while operating significantly fewer inference steps. The experimental results show that the student retains most of the reconstruction quality while achieving the teacher under the denoising stage evaluation protocol. The proposed framework incorporates the identity anchoring and temporal regularisation to identify the drift and frame-to-frame flicker during generation. Primarily CPU-only measurements and the edge computing measurements further indicate the few-step diffusion inference can be computationally feasible at reduced resolutions.

Although the present work primarily focuses on the feasibility and denoising stage metrics, it further evaluates standard perceptual audiovisual synchronisation metrics. Future direction of the work will be extended to further evaluate the full end-to-end video quality, improving the temporal stability metrics and cross-identity validation.

References

- [1] K. R. Prajwal, R. Mukhopadhyay, V. P. Namboodiri, and C. V. Jawahar, “A Lip Sync Expert Is All You Need for Speech to Lip Generation in the Wild,” in *Proceedings of the ACM International Conference on Multimedia (ACM Multimedia)*, 2020.
- [2] A. Roy, B. S. Gyanchandani, J. Sahu, and K. Mallikharjuna Rao, “SyncNet: Harmonizing Nodes for Efficient Learning,” in *2024 International Conference on Software, Telecommunications and Computer Networks (SoftCOM)*, 2024, pp. 1–6. doi:10.23919/SoftCOM62040.2024.10721994.
- [3] Y. Zhou, X. Han, E. Xie, et al., “MakeItTalk: Speaker-Aware Talking-Head Animation,” in *Proceedings of the ACM International Conference on Multimedia (ACM Multimedia)*, 2020.
- [4] W. Zhang, X. Cun, X. Wang, Y. Zhang, X. Shen, Y. Guo, Y. Shan, F. Wang, “SadTalker: Learning Realistic 3D Motion Coefficients for Stylized Audio-Driven Single Image Talking Face Animation,” in *Proceedings of the IEEE/CVF Conference on Computer Vision and Pattern Recognition (CVPR)*, 2023.
- [5] S. Shen, et al., “DiffTalk: Crafting Diffusion Models for Generalized Audio-Driven Portraits Animation,” in *Proceedings of the IEEE/CVF Conference on Computer Vision and Pattern Recognition (CVPR)*, 2023.
- [6] J. Ho, A. Jain, and P. Abbeel, “Denoising Diffusion Probabilistic Models,” in *Advances in Neural Information Processing Systems (NeurIPS)*, 2020.
- [7] J. Song, C. Meng, and S. Ermon, “Denoising Diffusion Implicit Models,” in *International Conference on Learning Representations (ICLR)*, 2021.
- [8] R. Rombach, A. Blattmann, D. Lorenz, P. Esser, B. Ommer, “High-Resolution Image Synthesis with Latent Diffusion Models,” in *Proceedings of the IEEE/CVF Conference on Computer Vision and Pattern Recognition (CVPR)*, 2022.
- [9] C. Lu, Y. Zhou, F. Bao, J. Chen, C. Li, J. Zhu, “DPM-Solver: A Fast ODE Solver for Diffusion Probabilistic Model Sampling in Around 10 Steps,” in *Advances in Neural Information Processing Systems (NeurIPS)*, 2022.
- [10] C. Lu, Y. Zhou, F. Bao, J. Chen, C. Li, J. Zhu, “DPM-Solver++: Fast Solver for Guided Sampling of Diffusion Probabilistic Models,” in *International Conference on Learning Representations (ICLR)*, 2023.
- [11] Y. Song, P. Dhariwal, M. Chen, I. Sutskever, “Consistency Models,” *arXiv preprint arXiv:2303.01469*, 2023.
- [12] T. Yin, et al., “One-Step Diffusion with Distribution Matching Distillation,” in *Proceedings of the IEEE/CVF Conference on Computer Vision and Pattern Recognition (CVPR)*, 2024.
- [13] Z. Zhou, et al., “Simple and Fast Distillation of Diffusion Models,” in *Advances in Neural Information Processing Systems (NeurIPS)*, 2024.
- [14] T. Afouras, J. S. Chung, A. Zisserman, “LRS3-TED: A Large-Scale Dataset for Visual Speech Recognition,” *arXiv preprint arXiv:1809.00496*, 2018.
- [15] Z. Zhang, L. Li, Y. Ding, C. Fan, “Flow-Guided One-Shot Talking Face Generation with a High-Resolution Audio-Visual Dataset,” in *Proceedings of the IEEE/CVF Conference on Computer Vision and Pattern Recognition (CVPR)*, 2021.
- [16] R. Zhang, P. Isola, A. A. Efros, E. Shechtman, O. Wang, “The Unreasonable Effectiveness of Deep Features as a Perceptual Metric,” in *Proceedings of the IEEE/CVF Conference on Computer Vision and Pattern Recognition (CVPR)*, 2018.

- [17] T. Unterthiner, S. van Steenkiste, K. Kurach, R. Marinier, M. Michalski, S. Gelly, “FVD: A New Metric for Video Generation,” in *International Conference on Learning Representations (ICLR) Workshop*, 2019.
- [18] Raspberry Pi Ltd., “Raspberry Pi 4 Model B Product Brief,” Product Brief, February 2026.
- [19] Raspberry Pi Ltd., “Raspberry Pi 4 Model B Product Page,” Accessed 2026.
- [20] J. Ho, A. Jain, P. Abbeel, “Denoising Diffusion Probabilistic Models,” in *Advances in Neural Information Processing Systems 33 (NeurIPS 2020)*, 2020. [Online]. Available: <https://proceedings.neurips.cc/paper/2020/hash/4c5bcfec8584af0d967f1ab10179ca4b-Abstract.html>
- [21] M.-M. Cheng, T. Hu, F. Khan, L. Li, S. Li, T. Liu, J. Van De Weijer, Y. Wang, J. Yang, S. Yang, “Faster diffusion: Rethinking the role of the encoder for diffusion model inference,” in *NeurIPS 2024*, 2024. doi:10.52202/079017-2706.
- [22] V. K. Rakesh, S. Mazumdar, S. Pal, A. Das, T. Samanta, “Advancements in talking head generation: a comprehensive review of techniques, metrics, and challenges,” *The Visual Computer*, vol. 42, no. 1, Dec. 2025. doi:10.1007/s00371-025-04232-w.
- [23] A. Blattmann, R. Rombach, H. Ling, T. Dockhorn, S. W. Kim, S. Fidler, K. Kreis, “Align Your Latents: High-Resolution Video Synthesis with Latent Diffusion Models,” in *CVPR 2023*, Vancouver, BC, Canada, 2023, pp. 22563–22575. doi:10.1109/CVPR52729.2023.02161.
- [24] Y. Song, P. Dhariwal, M. Chen, I. Sutskever, “Consistency Models,” in *ICML 2023*, Honolulu, Hawaii, 2023, vol. 202, pp. 32211–32252.
- [25] J. Song, C. Meng, S. Ermon, “Denoising Diffusion Implicit Models,” in *ICLR 2021*, Virtual Event, Austria, 2021.
- [26] S. Koyejo, S. Mohamed, A. Agarwal, D. Belgrave, K. Cho, A. Oh (Eds.), *Advances in Neural Information Processing Systems 35: NeurIPS 2022*, New Orleans, LA, USA, 2022.
- [27] T. Karras, M. Aittala, T. Aila, S. Laine, “Elucidating the Design Space of Diffusion-Based Generative Models,” in *NeurIPS 2022*, New Orleans, LA, USA, 2022.
- [28] P. Dhariwal, A. Q. Nichol, “Diffusion Models Beat GANs on Image Synthesis,” in *NeurIPS 2021*, pp. 8780–8794.
- [29] A. Q. Nichol, P. Dhariwal, “Improved Denoising Diffusion Probabilistic Models,” in *ICML 2021*, vol. 139, pp. 8162–8171.
- [30] S. Issabayeva, A. Katyetova, “Deep Learning of AI: Kazakhstan’s Case,” in *Advances in Information and Communication*, 2025, pp. 586–602.
- [31] T. Karras, M. Aittala, T. Aila, S. Laine, “Elucidating the Design Space of Diffusion-Based Generative Models,” *CoRR abs/2206.00364*, 2022. doi:10.48550/ARXIV.2206.00364.
- [32] T. Rice, “Real Time Inference on Raspberry Pi 4 and 5 (40 FPS!),” PyTorch Tutorials, 2025.
- [33] M. N. Jacob, “Power-Aware Image Classification on a Low-Cost Edge SBC: a reproducible Micro-Benchmark with MobileNetV3-Small and ResNet-18,” *TechRxiv*, Oct. 2025. doi:10.36227/techrxiv.176187020.04189831/v1.
- [34] Microsoft, “ONNX Runtime Performance Profiling Tools and onnxruntime_perf_test,” ONNX Runtime Documentation, Accessed 2026.

Author contributions

Soumya Mazumdar came up with the methodology, wrote the core algorithms, ran experiments, came up with theories, tested them, and wrote the first draft of the manuscript. **Vineet Kumar Rakesh** independently verified the experimental results and analyses to ensure technical accuracy and consistency. All of the authors looked over and approved the final draft.

Acknowledgments

The authors gratefully acknowledge the support provided by the Variable Energy Cyclotron Centre (VECC), the Department of Atomic Energy (DAE), and the Government of India (GoI) for granting access to the necessary infrastructure, tools, and technical assistance that enabled this research. We also extend our appreciation to the staff of the VECC library for their assistance and support throughout the course of this study.

Declaration of Competing Interest

All authors assert that they have no financial or personal connections that could be construed as affecting the work presented in this study. There are no conflicts of interest.

Data Availability Statement

The datasets used in this study are publicly available. The primary experiments were conducted using the LRS3-TED dataset, and the HDTF dataset is referenced as a standard benchmark for talking-head generation research. The raw datasets are not redistributed by the authors and should be obtained from their official sources subject to the respective licensing and usage terms. The code, preprocessing details, and experimental configuration associated with this work are available, or will be made available, through the project repository: <https://mazumdarsoumya.github.io/TempoSyncDiff>.

Author Biographies



Soumya Mazumdar is pursuing a dual degree: a B.Tech in Computer Science and Business Systems from Gargi Memorial Institute of Technology, and a B.S. in Data Science from the Indian Institute of Technology Madras. He has contributed to interdisciplinary research with over 25 publications in journals and edited volumes by Elsevier, Springer, IEEE, Wiley, and CRC Press. His research interests include artificial intelligence, machine learning, 6G communications, healthcare technologies, and industrial automation.



Vineet Kumar Rakesh is a Technical Officer (Scientific Category) at the Variable Energy Cyclotron Centre (VECC), Department of Atomic Energy, India, with over 22 years of experience in software engineering, database systems, and artificial intelligence. His research focuses on talking head generation, lipreading, and ultra-low-bitrate video compression for real-time teleconferencing. He is pursuing a Ph.D. at Homi Bhabha National Institute, Mumbai. Mr. Rakesh has contributed to office automation, OCR systems, and digital transformation projects at VECC. He is an Associate Member of the Institution of Engineers (India) and a recipient of the DAE Group Achievement Award.